Plasmodium vivax infection compromises reticulocyte stability.

Martha Clark
Harvard University
Usheer Kanjee
Harvard University
Gabriel Rangel
Pennsylvania State University University Park : Penn State
Laura Chery
University of Washington
Anjali Mascarenhas
Goa Medical College and Hospital
Edwin Gomes
Goa Medical College and Hospital
Pradipsinh Rathod
University of Washington
Carlo Brugnara
Boston CHildren's Hospital https://orcid.org/0000-0001-8192-8713
Marcello Ferreira
Instituto de Ciencias Biomedicas da USP
Manoj Duraisingh (mduraisi@hsph.harvard.edu)
Harvard University https://orcid.org/0000-0001-8534-5515

Article

Keywords: Plasmodium vivax, reticulocyte stability, malaria, RBC

Posted Date: August 19th, 2020

DOI: https://doi.org/10.21203/rs.3.rs-53799/v1

Version of Record: A version of this preprint was published at Nature Communications on March 12th, 2021. See the published version at https://doi.org/10.1038/s41467-021-21886-x.

Abstract

The structural integrity of the host red blood cell (RBC) must be maintained for propagation of *Plasmodium spp.* during the disease causing blood-stage of malaria infection. *Plasmodium vivax* infection is restricted to reticulocytes. To assess the impact of *P. vivax* infection on reticulocyte stability, we developed a flow cytometry-based assay capable of measuring osmotic stability within heterogeneous RBC populations. We found that *P. vivax* preferred young reticulocytes are more osmotically stable than older reticulocytes and normocytes, and *P. vivax* infection decreased reticulocyte stability to levels observed for RBC disorders that cause hemolytic anemia. Moreover, *P. vivax* reticulocyte destabilization was more significant than *P. falciparum* normocyte destabilization. Finally, we found that *P. vivax* new permeability pathways contribute to the decreased osmotic stability of infected-reticulocytes. These results reveal a key vulnerability of *P. vivax* that could be manipulated to yield both *in vitro* culture and novel therapeutics.

Introduction

The unique biconcave shape and structural dynamics of red blood cells (RBCs) permit traversal of the circulatory system and the delivery of oxygen to tissues, and are determined by molecules that make up the RBC cytoskeleton and membrane transporters [1]. Naturally occurring polymorphisms in molecules such as PIEZO1 and Ankyrin-1, that disrupt cell volume regulation and cytoskeleton, are associated with the clinically-relevant RBC phenotypes of hereditary xerocytosis (HX) [2] and hereditary spherocytosis (HS), [3] respectively. These mutations manifest in structurally compromised RBCs with abnormal shapes (stomatocytes and spherocytes) and premature hemolysis *in vivo* [4]. A feature of these mutant RBCs is abnormal sensitivity to hypotonic challenge, which is decreased in HX and increased in HS.

During the *Plasmodium* spp. intra-erythrocytic developmental cycle (IDC), parasite remodeling alters the physiology of the host RBC. In the case of the most well studied of these parasites, *P. falciparum*, changes include disruption of the cytoskeleton by parasite proteins inserted into the RBC membrane [5] and increased plasma membrane permeability [6,7] that culminate in the infected RBC taking on a spherical shape [8]. These changes compromise the structural integrity of the host RBC, and consequently decrease the osmotic stability of *P. falciparum*-infected RBCs [6,7,9], while increasing the propensity of infected cells to be destroyed in circulation via clearance by the spleen as well as extravascular hemolysis [10].

Plasmodium vivax, the most globally widespread of the malaria parasites infecting humans [11], exhibits a strict tropism for reticulocytes, the youngest of circulating RBCs [12–14]. This is in contrast to *P. falciparum*, which also infects the mature normocyte RBC fraction. The absence of an *in vitro* culture system and appropriate experimental methods have impeded the study of how *P. vivax* impacts the structural integrity of the host reticulocyte. The reticulocyte compartment itself is highly heterogeneous due to the dynamic final steps of RBC maturation, which involves enucleation, continued synthesis of hemoglobin, loss of membrane and organelles, and reconfiguration of the cytoskeleton [15–23]. All *P. falciparum* studies have

been done in the older, more abundant normocyte fraction. Furthermore, recent observations that *P. vivax* increases reticulocyte deformability [13,24,25] while *P. falciparum* decreases normocyte deformability [5,24,26] suggest that the pathophysiology of *P. vivax* reticulocyte infection are fundamentally different than *P. falciparum* normocyte infection.

Characterizing RBC stability under osmotic stress is a powerful method for probing the structural integrity of the cytoskeleton and membrane transporter activity, and therefore is invaluable for assessing RBC disorders that compromise *in vivo* fitness such as HS [2–4]. Reticulocytes [27–29] and erythroid progenitors [30] are more resistant to hypotonic lysis than normocytes, but the dynamics of osmotic stability during erythropoiesis and reticulocyte maturation are unknown. Osmotic stability is traditionally assessed by measuring release of hemoglobin from bulk RBC preparations in increasingly hypotonic solutions. This methodology cannot resolve the osmotic stability of specific RBC subpopulations within heterogeneous RBC preparations. Furthermore, using free hemoglobin as the read-out for RBC osmotic stability is problematic as hemoglobin levels are in flux in both parasite-infected RBCs and uninfected reticulocytes, because *Plasmodium* spp. digest hemoglobin as they mature [31], and reticulocytes are actively synthesizing hemoglobin [32]. Flow cytometry, with its ability to examine discrete cell subsets within heterogeneous populations, has the potential to better define RBC osmotic stability. Previous studies have demonstrated the capacity of flow cytometry to detect hemolysis [33–36], but are not amendable to collecting sufficient data on rare cell populations.

Here we have developed a flow cytometric osmotic stability assay that quantifies the RBCs that survive hypotonic lysis, and we have used it to assess the osmotic stability dynamics of reticulocytes and erythroid progenitors and the impact of *P. vivax* infection on reticulocyte osmotic stability. We found that osmotic stability steadily decreased during erythroid differentiation and reticulocyte maturation. Of enucleated RBCs the youngest CD71 + reticulocytes, preferred by *P. vivax*, are the most osmotically stable, but upon infection with *P. vivax* were destabilized to levels observed for RBCs from individuals with hemolytic anemia. Furthermore, *P. vivax*-infected reticulocytes were significantly less stable than *P. falciparum*-infected normocytes. Finally, we found that the decreased stability of *P. vivax*-infected reticulocytes corresponded with the appearance of *P. vivax* new permeability pathways (NPPs). In summary, by establishing an osmotic stability assay capable of assessing RBCs at the single cell level, we have been able to define the osmotic stability dynamics within heterogeneous reticulocyte and malaria-infected RBC populations. The observation that reticulocyte osmotic stability is reduced by *P. vivax* infection reveals a key vulnerability of the parasite.

Results

Flow cytometry analysis of RBC osmotic stability. While flow cytometry has been employed to study osmotic stability, previous studies have not harnessed the capacity of flow cytometry to analyze multiple cell populations within a single specimen [33–36]. Therefore we developed a flow cytometric osmotic stability assay that yields the same hemolysis curves as the traditional hemoglobin absorbance assay

and is capable of defining osmotic stability dynamics within heterogeneous RBC populations. Hemolysis curves were generated by first stopping lysis of RBCs in increasingly hypotonic solutions with a lysis quenching solution consisting of PBS and cell counting beads (Fig. 1A). This analysis revealed typical RBC forward scatter (FSC) and side scatter (SSC) profiles for non-lytic isotonic conditions, and the subsequent appearance of a low-FSC/low-SSC population in hypotonic, lytic conditions (Fig. 1B **and Supplemental Fig. 1**).

Hypothesizing that the low-FSC/low-SSC population was RBC ghosts, fluorescent phalloidin, which is excluded from intact cells but binds actin in the cytoskeleton of permeabilized cells was included in the osmotic stability assay. We found that phalloidin stained the FSC-low population that appears in lytic conditions, indicating that the flow lysis assay is sensitive to RBC ghosts (Fig. 1C and 1D). The FSC-low/SSC-low RBC ghost population was subsequently excluded when quantifying RBC osmotic stability. With this strategy the lysis curves produced by the flow lysis assay were indistinguishable from those of the hemoglobin absorbance lysis assay (Fig. 1E). No difference in the $lysis_{50}$ values (mOsm at which 50% of RBCs lyse) obtained for normal RBCs using the two lysis assays confirmed the accuracy of the flow lysis assay. To test the limits of the flow lysis assay, we measured the osmotic stability of hereditary xerocytosis (HX) RBCs that are resistant to hypotonic lysis. With HX RBCs as well, we observed no difference in $lysis_{50}$ values generated by the two assays (Fig. 1F).

Finally, as *P. vivax* osmotic stability studies included cryopreserved samples and were performed on RBCs maintained *in vitro*, we examined the effect of (i) cold storage and (ii) *P. vivax in vitro* culture conditions on RBC osmotic stability. As expected [37,38], we observed variation in the osmotic stability of normal RBCs taken from twelve different donors with $lysis_{50}$ values ranging from 93.9 to 137.9 mOsm (variation of 11.2%) (Fig. 1G). Subsequent storage of RBCs from six different donors at 4ºC for two weeks resulted in no appreciable change (mean slope − 0.063 ±0.24 SEM, Pearson r = 0.16) in osmotic stability (Fig. 1H). However, when cryopreserved RBCs and RBCs stored at 4ºC were transferred to *P. vivax in vitro* culture conditions, 24 hours later osmotic stability increased by 13% ±2.6 and 14.6% ±0.8 (Fig. 1I).

Osmotic stability decreases during erythroid differentiation and reticulocyte maturation.

Having established the capacity of flow cytometry to measure RBC osmotic stability, we next examined the osmotic stability dynamics within the RBC fractions that harbor *P. vivax* infection. To this end, we took advantage of the capacity of flow cytometry to track discrete cell populations, to assess the osmotic stability of nucleated RBC precursors, reticulocytes, and normocytes in bone marrow aspirates (Fig. 2A **and Supplemental 2A**). We found that fluorescent labeling of reticulocytes and nucleated RBC precursors present within bone marrow aspirates allowed us to quantitate the osmotic stability dynamics of each of these RBC subpopulations simultaneously (Fig. 2B). For nucleated RBC precursors we additionally found that lysed cells were also identifiable with a live/dead stain (**Supplemental 2B**). Importantly, as both osmotic stability studies with bone marrow aspirates and clinical *P. vivax* samples relied on Percoll enrichment to raise reticulocytemia and *P. vivax* parasitemia to reliably measurable levels, we found that

Percoll had no effect on the osmotic stability of reticulocytes and nucleated precursors from bone marrow aspirates (**Supplemental 2C**).

The $lysis_{50}$ values obtained for RBC precursors and reticulocytes from bone marrow aspirates revealed that nucleated RBC precursors (DNA + CD71+) were the most osmotically stable ($Lysis_{50}$ 70.1 ±5.8) followed by the youngest CD71 + RNA + DNA- reticulocytes ($Lysis_{50}$ 87.3 ±8.0), older CD71- RNA + DNA- reticulocytes ($Lysis_{50}$ 107.4 ±7.3) and CD71- RNA- DNA- normocytes ($Lysis_{50}$ 114.5 ±5.4) (Fig. 2B and 2C). To establish osmotic stability dynamics during erythropoiesis, we assessed the osmotic stability of erythroid progenitors differentiated *in vitro* from CD34 + stem cells [28,39]. This study revealed that osmotic stability decreased as cells progressed *in vitro* from majority basophilic and polychromatic normoblasts at day 9 ($Lysis_{50}$ 73.8 ±3.6) to a majority polychromatic and orthochromatic normoblast population at day 11 ($Lysis_{50}$ 102.7 ±15.6), and then further decreased as cells progressed through final orthochromatic normoblast maturation occurring between day 14 ($Lysis_{50}$ 102.2 ±2.0) day 17 ($Lysis_{50}$ 126.2 ±11.2), and day 20 ($Lysis_{50}$ 143.4 ±15.1) (Fig. 2D). Additionally, consistent with a previous study [28], CD71 + reticulocytes generated *in vitro* ($Lysis_{50}$ 110.1 ±3.7) were less stable than CD71 + reticulocytes from bone marrow samples ($Lysis_{50}$ 87.3 ±8.0) (**Supplemental Fig. 2D**). Together these results demonstrate the capacity of flow cytometry to assess the osmotic stability of discrete RBC subsets within heterogeneous populations and clearly shows that erythroid development and reticulocyte maturation are associated with significant changes in osmotic stability.

P. vivax **infection reduces reticulocyte osmotic stability.**

Having established that the youngest CD71 + reticulocytes that are preferred by *P. vivax* for invasion [13,14] are the most osmotically stable of all enucleated RBCs, we next assessed the impact of *P. vivax* infection on reticulocyte osmotic stability. In the absence of continuous *P. vivax in vitro* culture, cryopreserved clinical *P. vivax* samples are an invaluable resource for investigating *P. vivax* biology [40–43]. Cognizant of the decreased stability of cryopreserved RBCs, however (Fig. 1I), we first directly compared the *in vitro* survival and osmotic stability of cryopreserved and non-cryopreserved *P. vivax* clinical samples as parasites progressed through the IDC (Fig. 3A **and B and Supplemental Fig. 3A)**. Consistent with previous studies [40–43], we observed a 78% ±3.3 and 63% ±30.8 loss of *P. vivax* infected-reticulocytes prior to completion of the IDC *in vitro* (44-hour cultures) for Brazilian cryopreserved and Indian non-cryopreserved clinical samples respectively (Fig. 3C).

Parallel osmotic stability measurements revealed that, as observed previously (Fig. 1I), the stability of cryopreserved uninfected RBC populations increased upon transfer to *in vitro* culture, while non-cryopreserved uninfected RBCs remained steady during the course of culture (**Supplemental Fig. 3B and 3C**). For *P. vivax*-infected reticulocytes, we observed that cryopreserved stage I ring-infected reticulocytes were less stable than non-cryopreserved stage I rings. For subsequent time points we observed (i) no difference in the osmotic stability of cryopreserved and non-cryopreserved *P. vivax*-infected reticulocytes, and (ii) a decrease in the stability of *P. vivax*-infected reticulocytes as they progressed through the IDC

(Fig. 3D). Moreover, when we consider the clinical laboratory cutoff for normal RBCs ($lysis_{50}$171 mOsm or 0.5% NaCl), the osmotic stability of both cryopreserved and non-cryopreserved *P. vivax*-infected reticulocytes in 24- and 44-hour cultures fell into the range of osmotic stabilities associated with hemolytic anemias. Finally, in order to take advantage of the availability of cryopreserved *P. vivax* clinical samples while also minimizing the influence of cryopreservation, we excluded the 1-hour post thaw time point from subsequent analysis.

We next examined the degree of instability *P. vivax* induced in the host reticulocyte by comparing the osmotic stability of CD71- and CD71 + *P. vivax*-infected reticulocytes to that of uninfected CD71 + reticulocytes. Due to reticulocyte maturation [44], this analysis was limited to the first 24-hours of *in vitro* culture, as the frequency of CD71 + *P. vivax*-infected and uninfected reticulocytes respectively decreased by 56% ±8.0 and 64% ±3.5 between 1 and 24-hours of culture, and then fell below the limit of detection (0.05% CD71 + reticulocytes) between 24 and 44 hours. Of note, the persistence of *P. vivax*-infected CD71 + reticulocytes in our *ex vivo* cultures through 24 hours (**Supplemental Fig. 3D and 3E**) is longer than previously observed for CD71 + cord blood reticulocytes invaded *in vitro* by *P. vivax* [13]. The reason for this discrepancy is not immediately evident and therefore subject for future investigation. We found infected reticulocytes were less stable than uninfected CD71 + reticulocytes at all-time points assessed (8-, 16-, and 24-hour cultures), and the progression of *P. vivax* through the IDC further decreased reticulocyte osmotic stability with the appearance of stage III late trophozoite forms in 24-hour cultures corresponding to *P. vivax*-infected CD71 + and CD71- reticulocytes being 71.4% ±12.0 and 74.0% ±14.6 less stable than uninfected CD71 + reticulocytes (Fig. 3D). Finally no difference in the stability of CD71 + and CD71- infected-reticulocytes indicated that *P. vivax* infection and not reticulocyte age is the primary determinate of the stability of *P. vivax*-infected reticulocytes (**Supplemental Fig. 3F**).

P. vivax **induces greater host cell instability than** P. falciparum

Finally we compared *P. vivax* destabilization of reticulocytes with *P. falciparum* destabilization of normocytes. To account for the influence of cryopreservation on our *P. vivax* osmotic stability studies, we assessed the *in vitro* survival and osmotic stability of cryopreserved *P. falciparum* clone *3D7* P2G12 [45]. We observed similar progression of *P. vivax* and *P. falciparum* through the asexual IDC but a greater frequency of sexual gametocyte forms for *P. vivax*. *In vitro* survival, however, was markedly different, with a 77.3% ±6.5 survival rate observed for *P. falciparum* infected-normocytes at 44-hours of culture compared to a 22.4% ±0.03 survival rate for *P. vivax* infected-reticulocytes (Fig. 3C and 3F).

We subsequently assessed the osmotic stability of uninfected and *P. falciparum* trophozoite and schizonts stage-infected normocytes in 24- and 44-hour cultures (the points at which *P. vivax*-infected reticulocytes were most destabilized). This analysis revealed no difference in the osmotic stability of infected (majority trophozoite) and uninfected normocytes in 24-hour cultures and a reduction in infected normocyte (majority schizonts) stability of 23.6% ±6.9 compared to uninfected normocytes in 44 hour cultures (Fig. 3G). This is in contrast to *P. vivax*, which had decreased reticulocyte stability by 74.0% ±14.6 by the time parasites had matured to the trophozoite form in 24 hour cultures. Furthermore, direct

comparison of the osmotic stability of *P. falciparum*-infected normocytes and *P. vivax*-infected reticulocytes revealed that *P. vivax*-infected reticulocytes (max $Lysis_{50}$ 184.1 ±8.3, 24-hour culture) are significantly less stable, $p < 0.0003$, than *P. falciparum*-infected normocytes (max $Lysis_{50}$ 107.8 ±4.7, 44-hour culture) (Fig. 3H).

Appearance of P. vivax **new permeability pathways corresponds with decreased stability of** P. vivax**-infected reticulocytes.**

New permeability pathways (NPPs) in related malaria parasites, *P. falciparum* and *P. knowlesi*, increase the permeability of the infected RBC to certain solutes [6,7]. To determine whether *P. vivax* possesses NPPs that are contributing to the decreased stability of the host cell, we assessed the sensitivity of Percoll-enriched cryopreserved Brazilian clinical *P. vivax* samples to the NPP antagonists D-sorbitol and L-alanine. We found that uninfected RBCs were not sensitive to D-sorbitol or L-alanine (data not shown). For *P. vivax*-infected reticulocytes, we found that early stage parasites present in 8-hour cultures were resistant to D-sorbitol and L-alanine lysis, while the appearance of stage III late trophozoite parasites in 16-hour cultures corresponded with *P. vivax*-infected reticulocytes lysing in isotonic D-sorbitol (16-hour – 47.9% ±9.0, 24-hour – 45.2% ±9.2, and 44-hour – 57.5% ±7.7) and L-alanine solutions (16-hour – 60.7% ±10.5, 24-hour – 61.0% ±9.2, and 44-hour – 55.8% ±2.3). Finally, the NPP inhibitor, furosemide, protected *P. vivax*-infected reticulocytes from D-sorbitol and L-alanine lysis (Fig. 4A and 4B). The incomplete lysis of *P. vivax*-infected cells by D-sorbitol and L-alanine along with variation in the sensitivity of different *P. vivax* clinical isolates to D-sorbitol and L-alanine lysis are potentially driven by (i) the high frequency of more stable gametocytes (42.4% ±9.5 of *P. vivax*-infected reticulocytes in 44-hour cultures) [46,47] (Fig. 3C), (ii) variable NPP activity in different *P. vivax* isolates, or (iii) *P. vivax* being less sensitive to D-sorbitol lysis than *P. falciparum*[48,49].

Discussion

Structural stability of *P. vivax*-infected reticulocytes, critical for the successful propagation of blood-stage malaria infections, has not been thoroughly assessed due to lack of appropriate methodology compatible with the unique and challenging biology of *P. vivax*. To study the impact of *P. vivax* infection on the structural integrity of the host reticulocyte, we adapted the osmotic stability assay to be analyzed by flow cytometry. This permitted us to work with the limited cell numbers and heterogeneity characteristic of both the reticulocyte niche to which *P. vivax* infection is restricted as well as *P. vivax*-infected clinical samples. Observations made in the proceeding studies that the youngest CD71 + reticulocyte subset, which *P. vivax* preferentially invades, was the most osmotically stable and that *P. vivax*-infected reticulocytes were less stable than uninfected CD71 + reticulocytes, indicate that *P. vivax* severely compromises the structural integrity of the host reticulocyte. The single-cell resolution of the flow cytometry osmotic stability assay has additional applications including: tracking the impact of erythropoiesis perturbations on overall RBC osmotic stability and examination of osmotic stability dynamics within heterozygous hematological diseases such as sickle cell and G6PD deficiency.

The decreasing osmotic stability we observed in the later stages of erythropoiesis and then continuing through reticulocyte maturation is likely driven by three major changes occurring to erythroid cells during their differentiation: (i) intracellular solutes changes due to changing membrane transporter abundance and activity [19,21], (ii) cytoskeleton remodeling [17,22], and (iii) the progressive reduction in the surface to volume ratio driven by membrane loss [23]. Considering previous reports of membrane instability in reticulocytes [50], one might hypothesize that reticulocytes would be less osmotically stable than normocytes. The observation of the opposite by us and others [27–29] indicates that either the factors that determine osmotic stability, such as the higher surface area to volume ratio and greater abundance and activity of membrane transporters in reticulocytes, are more dominant than reticulocyte membrane instability, or that the biology underlying membrane instability and osmotic stability are independent of one another. Ultimately, the factors that determine osmotic stability during erythropoiesis and reticulocyte maturation are likely multifactorial and highly dynamic. Despite the underlying complexity, recent observations of the importance of cholesterol for *in vitro* differentiated reticulocyte osmotic stability [28] suggest that pursuing the determinants of erythroid progenitor and reticulocyte osmotic stability has the potential to yield strategies for generating more viable RBCs from *in vitro* cultures.

Our study revealed that *P. vivax* infection decreased the osmotic stability of the host reticulocyte. Though consistent with what has been observed for other *Plasmodium* spp. [6,7,9,51,52], *P. vivax* decreased reticulocyte osmotic stability to a significantly greater degree than *P. falciparum* decreased normocyte osmotic stability and to a level on par with RBC instability observed for hemolytic anemias like HS. Interestingly *P. knowlesi*-infected normocytes have also been reported to be less stable than *P. falciparum*-infected normocytes[48]. Comparing this data set with ours however, we estimate *P. vivax*-infected reticulocytes are even less stable (70% less stable than *P. falciparum*-infected normocytes) than *P. knowlesi*-infected normocytes (30% less stable than *P. falciparum*-infected normocytes). These results, specifically the compromised stability of mature *P. vivax*-infected reticulocytes, are consistent with a study in which the majority of late stage *P. vivax*-infected reticulocytes lysed when passed through 2 μm microfluidic channels [25] and suggest that the instability induced by P. vivax significantly increases the risk of pre-mature hemolysis of infected reticulocytes *in vivo*. Considering these findings in the context of the protection from *Plasmodium* infection afforded by RBC polymorphisms such as HS, thalassemia, and G6PD deficiency, it is possible that a mechanism underlying protection from *P. vivax* may be premature hemolysis of infected RBCs.

The observation that *P. vivax* NPPs are associated with reduced stability of host reticulocytes raises several questions including: (i) are *P. vivax* NPPs required for the acquisition of essential nutrients from the host serum and (ii) what host and or parasite transporters are responsible for the observed NPP activity. In *P. falciparum*, Clag3.1 and Clag3.2 have been identified as parasite mediators of NPP activity in infected RBCs [53,54], and *P. vivax* possesses a *clag* family of genes [55]. Despite the aforementioned differences, the very presence of NPP activity in *P. vivax*-infected reticulocytes suggests some overlap between the underlying factors responsible for the reduced osmotic stability of *P. falciparum*- and *P. vivax*-infected cells.

Together our data support a model in which *P. vivax*-preferred CD71 + reticulocytes are more osmotically stable than CD71- reticulocytes and normocytes, but, upon *P. vivax* infection and subsequent maturation, the infected host cells undergo a precipitous loss of osmotic stability. Additionally, the onset of NPP activity corresponds with the decreasing osmotic stability of infected reticulocytes (Fig. 4C). Furthermore, the magnitude of instability induced by *P. vivax* is on par with the RBC instability observed for hemolytic anemias like HS. As a result, *P. vivax*-infected reticulocytes likely exhibit increased rates of intravascular hemolysis and premature clearance from circulation similar to what is observed for RBCs from individuals with hemolytic anemias. Future studies will focus on the mechanisms underlying these changes in osmotic stability that impact the structural integrity of the host reticulocyte and potentially its ability to survive *in vivo*. Furthermore, identifying strategies for stabilizing the *P. vivax*-infected reticulocyte could prove key to culture-adapting *P. vivax* [56]. An additionally intriguing focus of future work, is the identification of therapeutic strategies that take advantage of the decreased stability of *P. vivax*-infected reticulocytes.

Materials And Methods

Ethics approval:

Anonymized discarded human bone marrow samples negative for blasts or dis-erythropoietic conditions were obtained under Boston Children's Hospital Institutional Review Board (IRB) protocol # 04-02-017R. For Brazilian clinical *P. vivax* samples, informed consent was obtained from all patients. Study protocols for Brazilian parasite sample collection were approved by the IRB of the Institute of Biomedical Sciences, University of São Paulo, Brazil (1169/CEPSH, 2014). For Indian *P. vivax* samples, the human subject protocol was approved by the ethics boards at Goa Medical College and Hospital (no number assigned), the University of Washington (42271), and the Division of Microbiology and Infectious Diseases of the National Institutes of Health (11–0074). The overall research program, under which the Indian parasites were collected, was also approved by the Government of India Health Ministry Screening Committee.

Parasite Sample Collection

Brazilian clinical *P. vivax* samples were collected in the town of Mâncio Lima, Acre State, and processed as described elsewhere [57]. The collections were performed in the context of a randomized, open-label clinical trial (NCT02691910). Indian *P. vivax* samples were collected with similar protocols but using CF11 for leukodepletion, as described previously [58]. This occurred at Goa Medial College and Hospital in Bambolim, Goa, in conjunction with the Malaria Evolution in South Asia International Center of Excellence in Malaria Research and the University of Washington.

Bone marrow and parasite enrichment

Bone marrow aspirates, cryopreserved Brazilian clinical *P. vivax* samples and the *P. falciparum 3D7 P2G12* lab strain were enriched on 1.080 g/mL KCl high Percoll gradients as previously described [59]. Briefly, 2 mL of re-suspended cells (up to 25% hematocrit) were layered on 3 mL 1.080 g/mL KCl high

Percoll gradient and spun for 15 minutes at 1,200 x g. Subsequently, the interface was removed, washed, and applied to assays. For *P. falciparum* 3D7 P2G12 samples, the interface and pellet were washed and recombined before being applied to assays.

CD34 + in vitro RBC differentiation

CD34 + hematopoetic stem cells (HSCs) purchased commercially (Lonza) were differentiated *in vitro* following the previously described three-step differentiation protocol [28,39]. Giemsa-stained cytospins were prepared and 200 cells per slide (1000x magnification) were called as either proerythroblast, basophilic normoblast, polychromatic normoblast, orthochromatic normoblast or reticulocyte.

P. vivax and P. falciparum in vitro culture

Indian and Brazilian clinical *P. vivax* samples and *P. falciparum* 3D7 P2G12 were cultured at 100×10^6 cells per mL in IMDM (Gibco) containing 10% AB^+ heat-inactivated sera and 50 µg/mL gentamicin at 37ºC in 5% CO_2, 1% O_2, and 94% N_2 as previously described [40]. Hemacolor-stained cytospins were prepared and 200 cells per slide (1000x magnification) were called as either asexual stage (I-V) or gametocyte [60].

Flow Cytometry. For the described flow cytometry experiments, 1×10^7 cells were washed with flow buffer prior to staining with combinations of the following fluorophores: Thiazole Orange, 1:1000 (Thermo Fisher Scientific), Vybrant DyeCycle Violet, 1:5000 (Thermo Fisher Scientific) α-CD71-APC, 1:25 (Miltenyi Biotech), α-GypA-FITC, 1:100 (Stem Cell Technologies), Vybrant DyeCycle Green, 1:5000 (Thermo Fisher Scientific) and FITC-Phalloidin, 1:200 (Thermo Fisher Scientific). Bone marrow and *in vitro* cultured RBC samples were stained at 4ºC for 20 minutes and *P. vivax* and *P. falciparum* samples at 37ºC for 20 minutes. For bone marrow and *in vitro*-cultured cell samples, propidium iodide, 1:500 (Thermo Fisher Scientific) was added to samples prior to flow cytometry analysis. All flow cytometry experiments were acquired on a Miltenyi MACSQuant instrument equipped with 405-nm, 488-nm, and 638-nm lasers and data were analyzed using FlowJo (Version 10.4).

Osmotic stability assays. Lysis solutions were made as previously described [61] and the osmolarity of each was measured with a vapor pressure osmometer (Wescor Vapro 5520). For flow cytometric osmotic stability assays, 1×10^6 cells (stained with appropriate fluorescent dyes and or antibodies) at 5×10^6 cells/mL were incubated in lysis solutions ranging from ~ 300 mOsm to 0 mOsm (distilled water) for 10 minutes at 37ºC. Lysis was stopped with 4x volume of quenching solution (1:10 AccuCheck Counting Beads (Thermo Fisher Scientific) to flow buffer). Only cells with normal flow cytometric FSC/SSC profiles (as defined by the control 300 mOsm condition) were considered to be intact. For assays containing nucleated cells, nuclei and dead cells were excluded from the intact cell population. The ratio of beads to intact cells was used to calculate the absolute number of cells remaining in each lytic condition and percent lysis was determined by normalization to the 300 mOsm control condition (0% lysis). For hemoglobin absorbance osmotic stability assays, cells were lysed as described above before 4x volume

of flow buffer was added to stop lysis. Cells were pelleted and the absorbance (380, 415, 450, and 540 nm) of supernatants measured on a Spectramax M5 plate reader. The amount of hemoglobin present in supernatants was calculated by the Harboe method [62]. Percent lysis was determined by normalization to the 300 mOsm control condition (0% lysis).

RBC ghost assay. For RBC ghost detection by flow cytometry, FITC conjugated phalloidin was added to all lysis and quenching solutions. For RBC ghost detection by immunofluorescence microscopy, RBCs suspended in PBS containing FITC-Phalloidin were allowed to settle on a coverslip before a hypotonic solution (57 mOsm) containing FITC-Phalloidin was added and RBC lysis and ghost formation examined by live video microscopy on a Zeiss AxioObserver.Z1. Images were processed using Fiji software.

Sorbitol and Alanine hemolysis assay. 1×10^6 cells taken from *P. vivax* cultures were incubated for 30 minutes at 37^{o}C in flow buffer, 280 mM sorbitol with 1% BSA, or 280 mM alanine with 1% BSA in the presence or absence of 100 µM furosemide. Following incubation, cells were washed twice with flow buffer, and stained for flow cytometry analysis.

Data Sharing Statement. For original data, please contact mduraisingh@hsph.harvard.edu.

Declarations

Author Contributions

MAC UK GWR – Experimental design, execution and data analysis

LC, AM, EG, PKR, CB, MUF – Clinical management of uninfected and infected blood sample collection, including patient management and ethical clearance

MAC UK GWR CB MTD – Data interpretation and manuscript writing

Acknowledgments

This study was supported by U.S. NIH/NHLBI F32 HL136173, NIH R01 AI140751, NIH R01 HL139337 and NIH/NIAID MESA-ICEMR Program Project U19 AI89688, the Canadian Institutes of Health Research Postdoctoral Fellowship, and a Conselho Nacional de Desenvolvimento Científico e Tecnológico (CNPq) research scholarship. The clinical trial that originated samples from Brazil was supported by the Ministry of Health of Brazil and the CNPq, grant 404067/2012-3. The funders had no role in study design, data collection and interpretation, or the decision to submit the work for publication. The authors declare that they have no competing interests.

References

1. Uzoigwe, C. The human erythrocyte has developed the biconcave disc shape to optimise the flow properties of the blood in the large vessels. *Med. Hypotheses* **67**, 1159–1163 (2006).
2. Zarychanski, R. *et al.* Mutations in the mechanotransduction protein PIEZO1 are associated with hereditary xerocytosis. *Blood* **120**, 1908–1915 (2012).
3. Eber, S. W. *et al.* Ankyrin-1 mutations are a major cause of dominant and recessive hereditary spherocytosis. *Nat. Genet.* **13**, 214–218 (1996).
4. King, M.-J. & Zanella, A. Hereditary red cell membrane disorders and laboratory diagnostic testing. *International Journal of Laboratory Hematology* **35**, 237–243 (2013).
5. Glenister, F. K., Coppel, R. L., Cowman, A. F., Mohandas, N. & Cooke, B. M. Contribution of parasite proteins to altered mechanical properties of malaria-infected red blood cells. *Blood* **99**, 1060–1063 (2002).
6. Ginsburg, H., Krugliak, M., Eidelman, O. & Ioav Cabantchik, Z. New permeability pathways induced in membranes of Plasmodium falciparum infected erythrocytes. *Molecular and Biochemical Parasitology* **8**, 177–190 (1983).
7. Lisk, G. & Desai, S. A. The Plasmodial Surface Anion Channel Is Functionally Conserved in Divergent Malaria Parasites. *Eukaryot Cell* **4**, 2153–2159 (2005).
8. Safeukui, I. *et al.* Retention of Plasmodium falciparum ring-infected erythrocytes in the slow, open microcirculation of the human spleen. *Blood* **112**, 2520–2528 (2008).
9. Lew, V. L., Macdonald, L., Ginsburg, H., Krugliak, M. & Tiffert, T. Excess haemoglobin digestion by malaria parasites: a strategy to prevent premature host cell lysis. *Blood Cells Mol. Dis.* **32**, 353–359 (2004).
10. Buffet, P. A. *et al.* The pathogenesis of Plasmodium falciparum malaria in humans: insights from splenic physiology. *Blood* **117**, 381–392 (2011).
11. Howes, R. E. *et al.* Global Epidemiology of Plasmodium vivax. *Am J Trop Med Hyg* **95**, 15–34 (2016).
12. Craik, R. A NOTE ON THE ERYTHROCYTES IN MALARIA. *The Lancet* **195**, 1110 (1920).
13. Malleret, B. *et al.* Plasmodium vivax: restricted tropism and rapid remodeling of CD71-positive reticulocytes. *Blood* **125**, 1314–1324 (2015).
14. Gruszczyk, J. *et al.* Transferrin receptor 1 is a reticulocyte-specific receptor for Plasmodium vivax. *Science* **359**, 48–55 (2018).
15. Chu, T. T. T. *et al.* Quantitative mass spectrometry of human reticulocytes reveal proteome-wide modifications during maturation. *Br. J. Haematol.* **180**, 118–133 (2018).
16. Malleret, B. *et al.* Significant biochemical, biophysical and metabolic diversity in circulating human cord blood reticulocytes. *PLoS ONE* **8**, e76062 (2013).
17. Griffiths, R. E. *et al.* The ins and outs of human reticulocyte maturation: autophagy and the endosome/exosome pathway. *Autophagy* **8**, 1150–1151 (2012).
18. Rapoport, S. M., Dubiel, W. & Müller, M. The mechanism of maturation-dependent breakdown of mitochondria in reticulocytes. *Acta Biol. Med. Ger.* **40**, 1277–1283 (1981).

19. Blanc, L. *et al.* The water channel aquaporin-1 partitions into exosomes during reticulocyte maturation: implication for the regulation of cell volume. *Blood* **114**, 3928–3934 (2009).
20. Liu, J., Guo, X., Mohandas, N., Chasis, J. A. & An, X. Membrane remodeling during reticulocyte maturation. *Blood* **115**, 2021–2027 (2010).
21. Pan, D. *et al.* K-Cl cotransporter gene expression during human and murine erythroid differentiation. *J. Biol. Chem.* **286**, 30492–30503 (2011).
22. Koury, S. T., Koury, M. J. & Bondurant, M. C. Cytoskeletal distribution and function during the maturation and enucleation of mammalian erythroblasts. *J. Cell Biol.* **109**, 3005–3013 (1989).
23. Mohandas, N. & Groner, W. Cell membrane and volume changes during red cell development and aging. *Ann. N. Y. Acad. Sci.* **554**, 217–224 (1989).
24. Suwanarusk, R. *et al.* The deformability of red blood cells parasitized by Plasmodium falciparum and P. vivax. *J. Infect. Dis.* **189**, 190–194 (2004).
25. Handayani, S. *et al.* High deformability of Plasmodium vivax-infected red blood cells under microfluidic conditions. *J. Infect. Dis.* **199**, 445–450 (2009).
26. Cranston, H. A. *et al.* Plasmodium falciparum maturation abolishes physiologic red cell deformability. *Science* **223**, 400–403 (1984).
27. Grimberg, B. T. *et al.* Increased reticulocyte count from cord blood samples using hypotonic lysis. *Exp. Parasitol.* **132**, 304–307 (2012).
28. Bernecker, C. *et al.* Cholesterol Deficiency Causes Impaired Osmotic Stability of Cultured Red Blood Cells. *Front Physiol* **10**, 1529 (2019).
29. Tada, K., Watanabe, Y. & Miyazawa, H. [Studies on the reticulocyte. I. The MCV, MCH, MCHC and osmotic fragility of the reticulocyte]. *Paediatr Jpn* **66**, 263–265 (1962).
30. Niskanen, E. & Cline, M. J. Differentiation of subpopulations of human and murine hemopoietic stem cells by hypotonic lysis. *J. Clin. Invest.* **65**, 285–289 (1980).
31. Rudzinska, M. A., Trager, W. & Bray, R. S. Pinocytotic uptake and the digestion of hemoglobin in malaria parasites. *J. Protozool.* **12**, 563–576 (1965).
32. Smith, D. W. Reticulocyte transfer RNA and hemoglobin synthesis. *Science* **190**, 529–535 (1975).
33. Ciepiela, O., Adamowicz-Salach, A., Zgodzińska, A., Łazowska, M. & Kotuła, I. Flow cytometric osmotic fragility test: Increased assay sensitivity for clinical application in pediatric hematology. *Cytometry B Clin Cytom* (2017) doi:10.1002/cyto.b.21511.
34. Yamamoto, A. *et al.* Flow cytometric analysis of red blood cell osmotic fragility. *J Lab Autom* **19**, 483–487 (2014).
35. Nobre, C. S., Silva, J. A., Jácomo, R. H., Nery, L. F. A. & Barra, G. B. Flow Cytometric Analysis of Erythrocytes Osmotic Fragility in Hereditary Spherocytosis: A Case-Controlled Study Evaluating the Best Anticoagulant, Sample Pre-Treatment and NaCl Concentration for Reliable Screening of this Red Blood Cell Membrane Disorder. *Cytometry Part B: Clinical Cytometry* **94**, 910–917 (2018).

36. Warang, P., Gupta, M., Kedar, P., Ghosh, K. & Colah, R. Flow cytometric osmotic fragility–an effective screening approach for red cell membranopathies. *Cytometry B Clin Cytom* **80**, 186–190 (2011).
37. Fischbach, F. T. *A manual of laboratory and diagnostic tests*. (Wolters Kluwer Health, 2015).
38. Godal, H. C., Elde, A. T., Nyborg, N. & Brosstad, F. The normal range of osmotic fragility of red blood cells. *Scand J Haematol* **25**, 107–112 (1980).
39. Giarratana, M.-C. *et al.* Ex vivo generation of fully mature human red blood cells from hematopoietic stem cells. *Nat. Biotechnol.* **23**, 69–74 (2005).
40. Rangel, G. W. *et al.* Enhanced Ex Vivo Plasmodium vivax Intraerythrocytic Enrichment and Maturation for Rapid and Sensitive Parasite Growth Assays. *Antimicrob. Agents Chemother.* **62**, (2018).
41. Rangel, G. W. *et al.* Plasmodium vivax transcriptional profiling of low input cryopreserved isolates through the intraerythrocytic development cycle. *PLoS Negl Trop Dis* **14**, (2020).
42. Borlon, C. *et al.* Cryopreserved Plasmodium vivax and cord blood reticulocytes can be used for invasion and short term culture. *Int. J. Parasitol.* **42**, 155–160 (2012).
43. T, F., Jm, S., Ce, C., Te, W. & Tt, S. Reticulocytes from cryopreserved erythroblasts support Plasmodium vivax infection in vitro. *Parasitol Int* **63**, 278–284 (2013).
44. Gronowicz, G., Swift, H. & Steck, T. L. Maturation of the reticulocyte in vitro. *J. Cell. Sci.* **71**, 177–197 (1984).
45. Buchholz, K. *et al.* A high-throughput screen targeting malaria transmission stages opens new avenues for drug development. *J. Infect. Dis.* **203**, 1445–1453 (2011).
46. Saul, A., Graves, P. & Edser, L. Refractoriness of erythrocytes infected with Plasmodium falciparum gametocytes to lysis by sorbitol. *Int. J. Parasitol.* **20**, 1095–1097 (1990).
47. Shaw-Saliba, K. *et al.* Infection of laboratory colonies of Anopheles mosquitoes with Plasmodium vivax from cryopreserved clinical isolates. *Int. J. Parasitol.* **46**, 679–683 (2016).
48. Liu, B. *et al.* Multimodal analysis of Plasmodium knowlesi-infected erythrocytes reveals large invaginations, swelling of the host cell, and rheological defects. *Cell Microbiol* **21**, (2019).
49. van Schalkwyk, D. A., Moon, R. W., Blasco, B. & Sutherland, C. J. Comparison of the susceptibility of Plasmodium knowlesi and Plasmodium falciparum to antimalarial agents. *J. Antimicrob. Chemother.* **72**, 3051–3058 (2017).
50. Waugh, R. E. Reticulocyte rigidity and passage through endothelial-like pores. *Blood* **78**, 3037–3042 (1991).
51. Fogel, B. J., Shields, C. E. & Von Doenhoff, A. E. The osmotic fragility of erythrocytes in experimental malaria. *Am. J. Trop. Med. Hyg.* **15**, 269–275 (1966).
52. Seed, T. M., Brindley, D., Aikawa, M. & Rabbege, J. Plasmodium berghei: Osmotic fragility of malaria parasites and mouse host erythrocytes. *Experimental Parasitology* **40**, 380–390 (1976).
53. Nguitragool, W. *et al.* Malaria parasite clag3 genes determine channel-mediated nutrient uptake by infected red blood cells. *Cell* **145**, 665–677 (2011).

54. Mira-Martínez, S. *et al.* Epigenetic switches in clag3 genes mediate blasticidin S resistance in malaria parasites. *Cell. Microbiol.* **15**, 1913–1923 (2013).
55. Dharia, N. V. *et al.* Whole-genome sequencing and microarray analysis of ex vivo Plasmodium vivax reveal selective pressure on putative drug resistance genes. *Proc. Natl. Acad. Sci. U.S.A.* **107**, 20045–20050 (2010).
56. Thomson-Luque, R., Adams, J. H., Kocken, C. H. M. & Pasini, E. M. From marginal to essential: the golden thread between nutrient sensing, medium composition and Plasmodium vivax maturation in in vitro culture. *Malar J* **18**, (2019).
57. Ladeia-Andrade, S. *et al.* Monitoring the Efficacy of Chloroquine-Primaquine Therapy for Uncomplicated Plasmodium vivax Malaria in the Main Transmission Hot Spot of Brazil. *Antimicrob. Agents Chemother.* **63**, (2019).
58. Sriprawat, K. *et al.* Effective and cheap removal of leukocytes and platelets from Plasmodium vivax infected blood. *Malar. J.* **8**, 115 (2009).
59. Sorette, M. P., Shiffer, K. & Clark, M. R. Improved isolation of normal human reticulocytes via exploitation of chloride-dependent potassium transport. *Blood* **80**, 249–254 (1992).
60. Lim, C. *et al.* Reticulocyte Preference and Stage Development of Plasmodium vivax Isolates. *J Infect Dis.* **214**, 1081–1084 (2016).
61. Beutler, E., Kuhl, W. & West, C. The osmotic fragility of erythrocytes after prolonged liquid storage and after reinfusion. *Blood* **59**, 1141–1147 (1982).
62. Harboe, M. A method for determination of hemoglobin in plasma by near-ultraviolet spectrophotometry. *Scand. J. Clin. Lab. Invest.* **11**, 66–70 (1959).

Figures

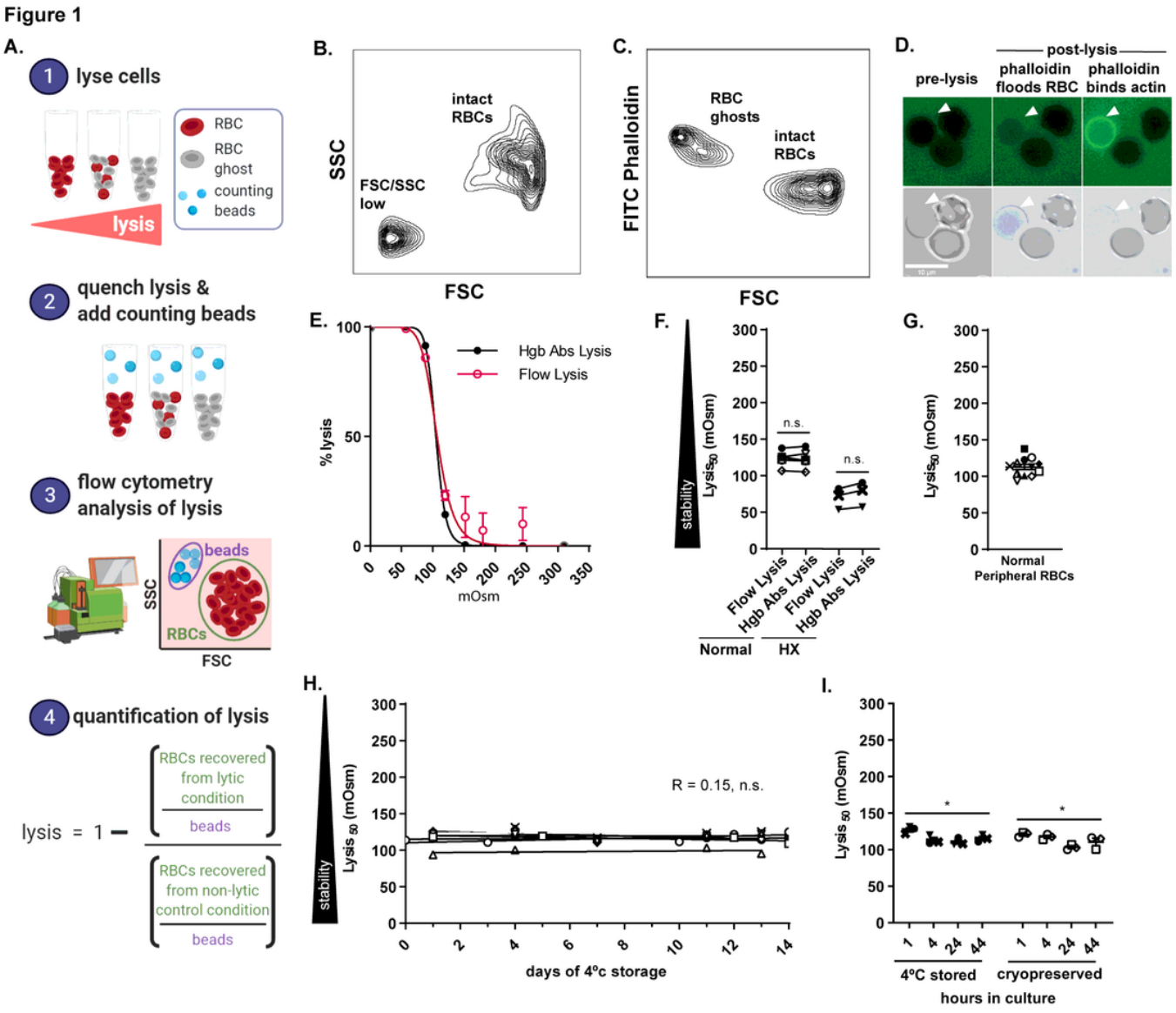

Figure 1

Development of a Flow Cytometry Osmotic Stability assay (A) Flow cytometry method for measuring RBC osmotic stability. (B) Representative flow cytometry forward scatter (FSC) by side scatter (SSC) plot of a lysed (120 mOsm) RBC sample. Data representative of 10 independent experiments. (C) Representative flow cytometry FSC by FITC-phalloidin plot of a lysed (120 mOsm) RBC sample. Data representative of five independent experiments. (D) Representative immunofluorescent images of FITC-phalloidin binding RBC ghosts. Scale bar, 10 μm. Arrows indicate a RBC undergoing lysis. Images were taken at 630x magnification on a Zeiss AxioObserver.Z1 inverted fluorescent microscope coupled to an AxioCam MRm camera. Images were processed using Fiji software. Data representative of two independent experiments. (E) Percent hemolysis of RBCs measured by hemoglobin absorbance osmotic stability assay (● ± SD), and flow cytometry osmotic stability assay (● ± SD). Data fit with least squares regression fit curves of normalized data. Data representative of five independent experiments. (F) Lysis50 values generated by flow cytometry and hemoglobin absorbance osmotic stability curves for normal (n=6) and HX (n=3) RBCs. Each unique symbol represents a different biological replicate and lines match the lysis50 values

obtained from flow cytometry and hemoglobin absorbance assays for that biological sample. Statistical significance between flow cytometry and hemoglobin absorbance lysis50 values assessed by student's t-test. (G) Lysis50 values for RBCs from 12 different donors as measured by flow cytometry. Each unique symbol represents a different biological replicate. Mean lysis50 value represented by horizontal line and SEM represented by error bars. (H) Lysis50 values for normal RBCs (n=6) sampled during the course of 14 days of 4 ºC storage. Each unique symbol represents a different biological replicate. Data fit with linear regression lines. Mean linear regression for all data depicted by solid line. Pearson r = 0.15, n.s. correlation between days of 4 ºC storage lysis50. (I) Lysis50 values for RBCs stored at 4ºC degrees (n=3) and cryopreserved (n=3) following transfer to P. vivax in vitro culture conditions. Osmotic stability assessed at 1-, 4-, 24-, and 44-hours of culture. Each unique symbol represents a different biological replicate. Mean Lysis50 values represented by horizontal lines and SEM represented by error bars. Statistical significance of Lysis50 changes during culture of cryopreserved and 4ºC degree stored RBCs assessed by ordinary one-way ANOVA analysis. *$p<0.02$.

Figure 2

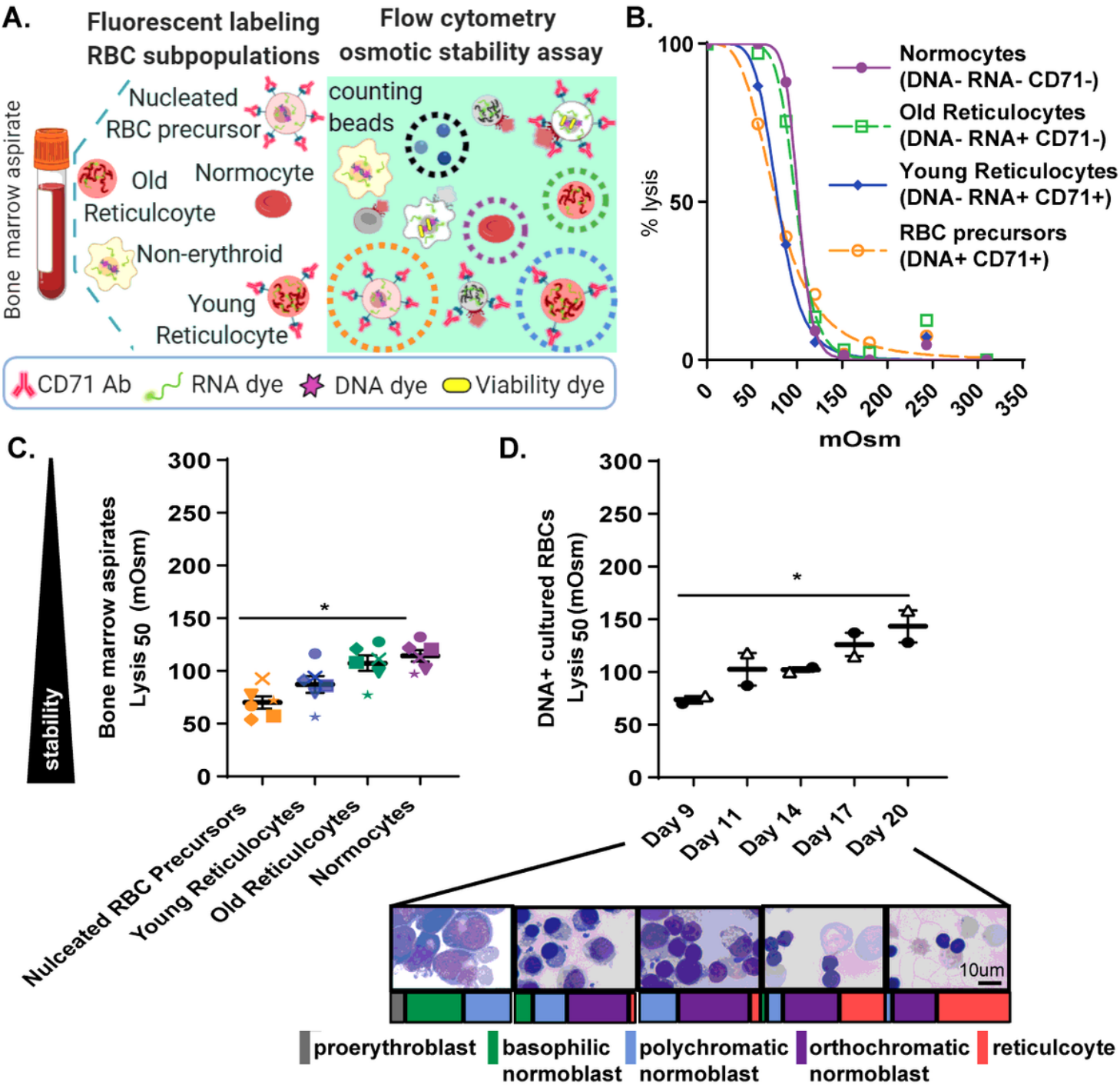

Figure 2

Osmotic stability dynamics during erythroid differentiation and reticulocyte maturation. (A) Flow cytometry method for measuring osmotic stability of RBC subpopulations. (B) Percent hemolysis of normocytes (DNA- RNA- CD71-), old reticulocytes (DNA- RNA+ CD71), young reticulocytes (DNA- RNA+ CD71+), and RBC precursors (DNA+ CD71+) from a bone marrow aspirate. Data fit with least squares regression fit curves of normalized data. Data representative of six biological replicates. (C) Lysis50 values for normocytes, old reticulocytes, young reticulocytes and RBC precursors in bone marrow

aspirates from 6 different donors. Each unique symbol represents a biological replicate (n=6). Mean Lysis50 values represented by horizontal lines and SEM represented by error bars. Statistical significance between the Lysis50 values of normocytes, reticulocytes, and erythroid precursors was assessed by ordinary one-way ANOVA analysis. *p<0.0006. (D) Lysis50 values for RBC progenitors differentiated in vitro from CD34+ stem cells. Unique symbols indicate the lysis50 values at days 9, 11, 14, 17 and 20 of two independent differentiations. Mean Lysis50 values represented by horizontal lines and SEM represented by error bars. Statistical significance of lysis50 changes during differentiation was determined by one-way ANOVA analysis. *p<0.04. Inset are representative photos of RBC progenitors during in vitro differentiation. Images were taken at 1000x magnification using an Excelis HD Camera attached to an Olympus BX40 microscope. Scale bar, 10 μm. Colored bars below images represent proportion of RBC progenitor developmental stages present at day 9, day 11, day 14, day 17, and day 20 of differentiation.

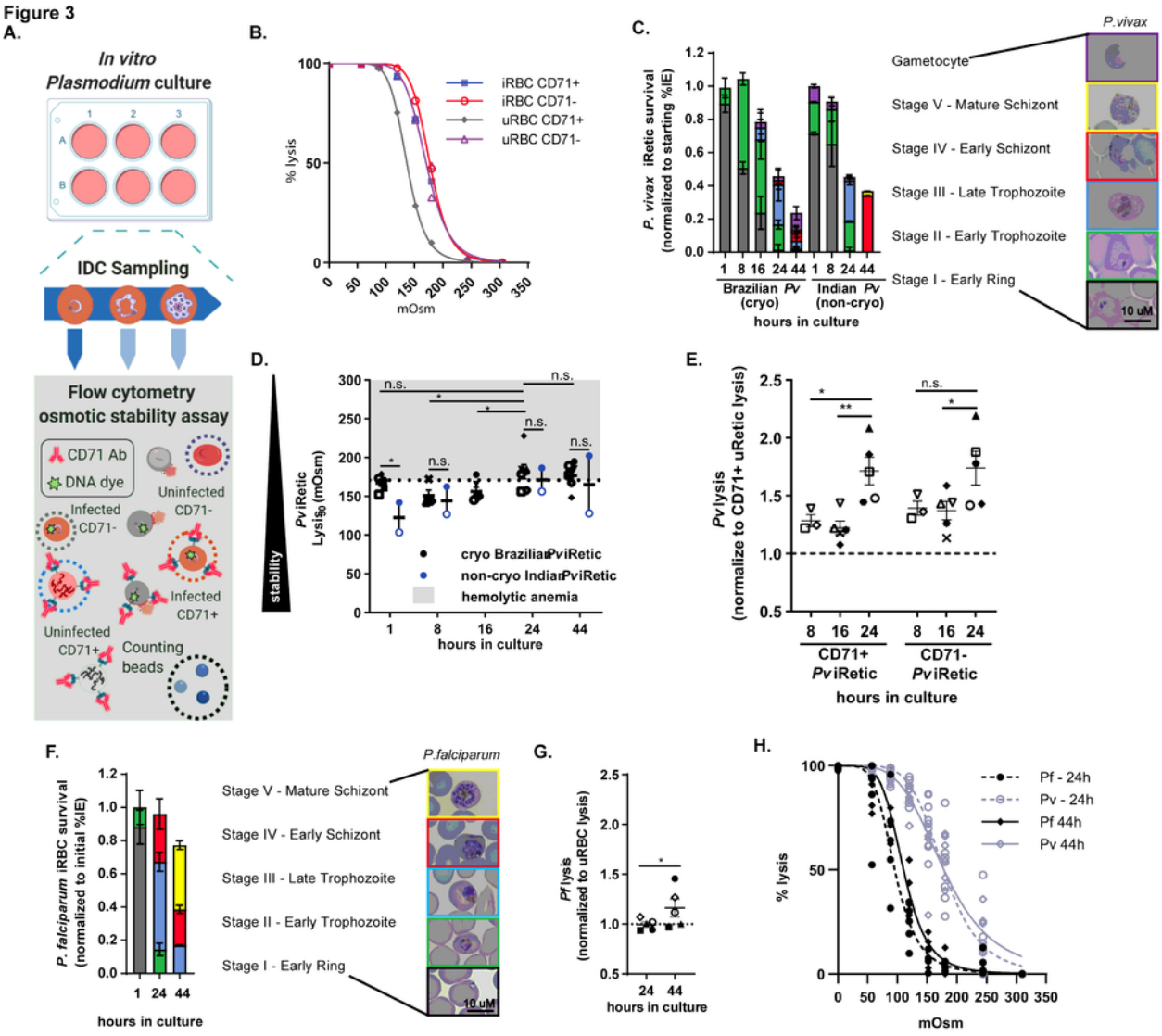

Figure 3

Osmotic stability of P. vivax-infected reticulocytes and P. falciparum-infected normocytes. (A) Strategy for measuring the osmotic stability of Plasmodium infected and uninfected RBC populations by flow cytometry. (B) Percent hemolysis of P. vivax infected CD71+ and CD71- reticulocytes (DNA+ CD71+ and DNA+ CD71-) and uninfected CD71+ reticulocytes (DNA- CD71+) and normocytes (DNA- CD71-) from a cryopreserved Brazilian clinical P. vivax sample after 1-hour of in vitro culture. Data fit with least squares

regression fit curves of normalized data. Data representative of six biological replicates. (C) Developmental stage of in vitro cultured ex vivo and cryopreserved P. vivax clinical isolates. Ex vivo data represents the mean of two ex vivo Indian P. vivax isolates. Cryopreserved data represents the mean of five cryopreserved Brazilian clinical P. vivax isolates. Error bars represent standard deviation. Inset are representative photos of P. vivax IDC development stages. Images were taken at 1000x magnification using an Excelis HD Camera attached to an Olympus BX40 microscope. Scale bar, 10 μm. (D) Lysis50 values P. vivax-infected reticulocytes from cryopreserved Brazilian and non-cryopreserved Indian clinical P. vivax samples after 1-, 8-, 16-, 24-, and 44-hours of in vitro culture. Each unique symbol denotes a different Brazilian or Indian P. vivax isolate. Mean lysis50 represented by horizontal line and SEM represented by error bars. Dashed line (171 mOsm) and gray shading indicate lysis50 values associated with hemolytic anemias. Statistical significance between lysis50 cryopreserved Brazilian and non-cryopreserved Indian P. vivax-infected reticulocytes assessed by student's t-test. *p<0.01 Statistical significance between cryopreserved Statistical significance between Brazilian P. vivax-infected reticulocytes at 24-hours of culture compared to 1-, 8-, 16- and 44-hours in vitro culture assessed by Dunnett's multiple comparisons test. *p<0.05. (E) P. vivax-infected CD71+ and CD71- lysis50 values normalized to lysis50 values of corresponding uninfected CD71+ reticulocytes at 1- (n=6), 8- (n=3), 16- (n=5), and 24-hours (n=5) of in vitro culture of cryopreserved Brazilian P. vivax isolates. Each unique symbol denotes a different Brazilian P. vivax isolate. Mean relative stability represented by horizontal lines and SEM represented by error bars. Statistical significance between normalized stability of P. vivax-infected CD71+ or CD71- reticulocytes at 24-hours of culture compared to 1-, 8- and 16-hours of culture assessed by student's t-test. *p<0.05 **p<0.01. (F) Developmental stage of in vitro-cultured, cryopreserved P. falciparum 3D7 P2G12 clone (n=5). Error bars represent the standard deviation. Inset are representative photos of P. falciparum IDC development stages. Images were taken at 1000x magnification using an Excelis HD Camera attached to an Olympus BX40 microscope. Scale bar, 10 μm. (G) P. falciparum-infected RBC lysis50 values normalized to lysis50 values of corresponding uninfected RBCs at 24- and 44-hours of in vitro culture of cryopreserved P. falciparum 3D7 P2G12 samples (n=5). Symbols denote biological replicates. Mean relative stability represented by horizontal lines and SEM represented by error bars. Statistical significance between normalized stability of P. falciparum-infected RBCs at 24-hours and 44-hours of culture assessed by student's t-test. *p<0.05. (H) Percent hemolysis of cryopreserved Brazilian P. vivax-infected reticulocytes (n=7) and P. falciparum 3D7 P2G12 clone infected-normocytes (n=5) after 24- and 44-hours of in vitro culture. Data points represent lysis values from biological replicates. Data fit with least squares regression fit curves of normalized data.

Figure 4

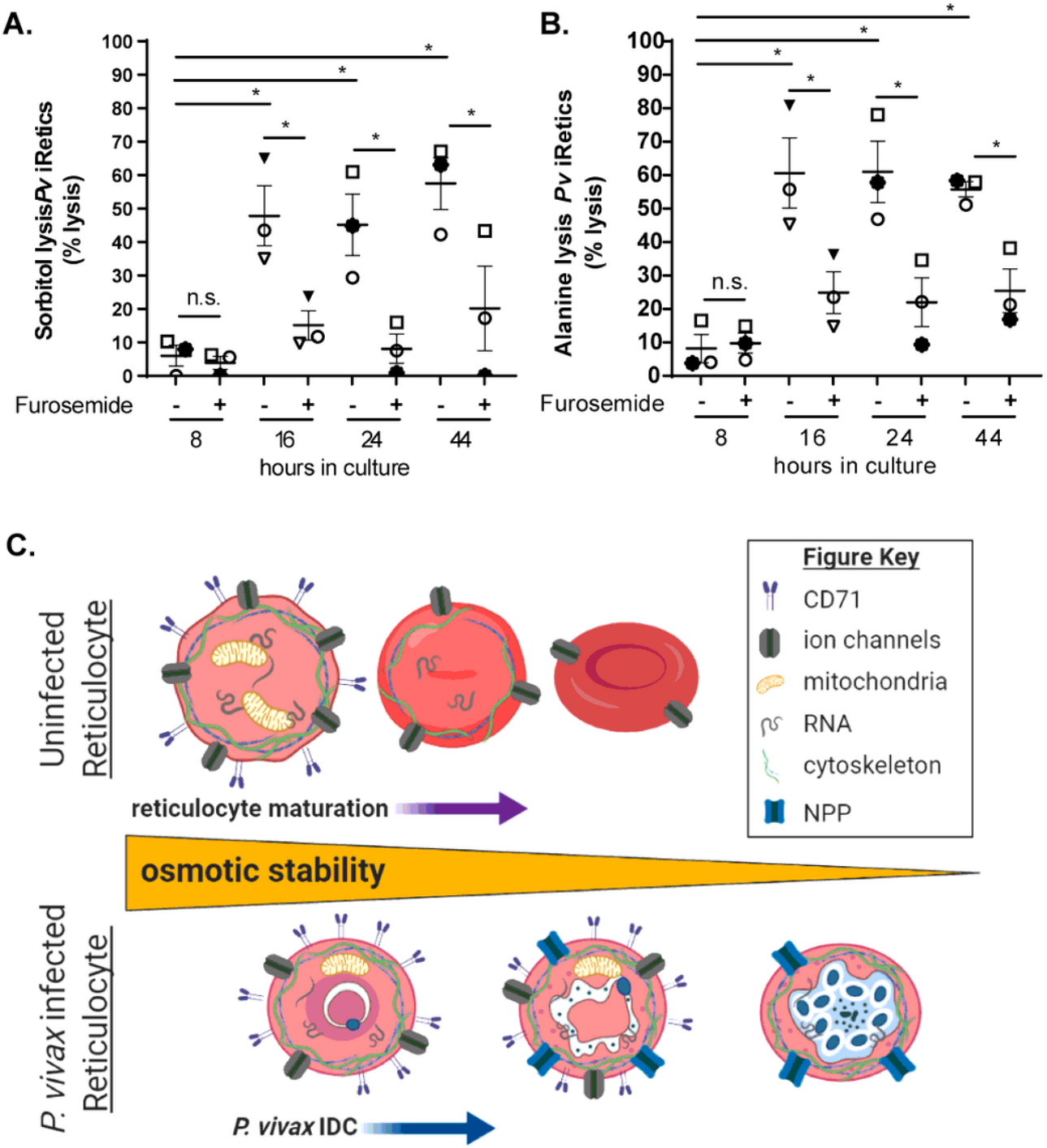

Figure 4

P. vivax new permeability pathways increase the permeability of P. vivax infected reticulocytes. Sensitivity of cryopreserved Brazilian P. vivax-infected reticulocytes to (A) D-sorbitol and (B) L-alanine lysis in the presence and absence of NPP inhibitor furosemide in 8- (n=3), 16- (n=3), 24- (n=3), and 44-hour (n=3) cultures post thaw. Each unique symbol denotes a different Brazilian P. vivax isolate. Mean % lysis represented by horizontal lines and SEM represented by error bars. Statistical significance between furosemide treated and untreated cells determined by student's t-test. *p<0.05. Statistical significance

between P. vivax-infected reticulocyte lysis at 8-hours of culture compared to 16-, 24- and 44-hours in vitro culture assessed by Dunnet's multiple comparisons test. *p<0.01. (C) Model of the osmotic stability dynamics within the reticulocyte compartment and the impact of P. vivax infection on reticulocyte osmotic stability.

Supplementary Files

This is a list of supplementary files associated with this preprint. Click to download.

- SupplementalFigures.docx